SURFACE RECOGNITION BY PARAMETRIC MODELING OF INFRARED INTENSITY SIGNALS

Tayfun Aytaç and Billur Barshan

Department of Electrical Engineering
Bilkent University
TR-06800 Bilkent, Ankara, Turkey
Tel: (90 312) 290-2161, Fax: (90 312) 266-4192
E-mail: {taytac, billur}@ee.bilkent.edu.tr

ABSTRACT

In this study, low-cost infrared emitters and detectors are used for the recognition of surfaces with different properties in a location-invariant manner. The intensity readings obtained with such sensors are highly dependent on the location and properties of the surface in a way that cannot be represented analytically in a simple manner, complicating the differentiation and localization process. Our approach, which models infrared intensity signals parametrically, can distinguish different surfaces independently of their positions. Once the surface type is identified, its position can also be estimated. The method is verified experimentally with wood, styrofoam packaging material, white painted wall, white and black clothes, and white, brown, and violet papers. A correct differentiation rate of 73% is achieved over eight surfaces and the surfaces are localized within absolute range and azimuth errors of 0.8 cm and 1.1°, respectively. The differentiation rate improves to 86% over seven surfaces and 100% over six surfaces. The method demonstrated shows that simple infrared sensors, when coupled with appropriate signal processing, can be used to extract a significantly greater amount of information than they are commonly employed for.

1. INTRODUCTION

In this study, surfaces having different colors and textures have been recognized by parametric modeling of infrared intensity scan signals. The proposed approach can differentiate a moderate number of surfaces and estimate their positions. In this section, the interaction of light with surfaces is briefly explained and some existing models are reviewed.

Light reflected from objects depends on the wavelength and distance of the light source, the properties of the light source (i.e., point or diffuse source), and the surface properties of the objects under consideration such as reflectivity, absorbtivity, transmittivity, and orientation [1, 2]. Depending on the surface properties, reflectance can be modeled in different ways:

Matte materials can be approximated as ideal Lambertian surfaces which absorb no light and reflect all the incident light with equal intensities in all directions with respect to the incidence angle [1, 3]. The intensity of the reflected light depends on the angle γ between the surface normal and the incident light (Fig. 1). When a Lambertian surface is illuminated by a point source of irradiance E, then the reflection function will be

$$\mathcal{R} = \frac{1}{\pi} E \cos(\gamma), \quad \text{for} \quad \gamma \geq 0, \tag{1}$$

which is known as "cosine" or Lambert's law of reflection from matte surfaces [3].

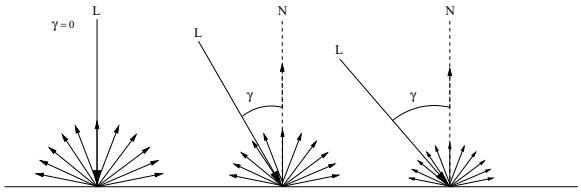

Figure 1: Diffuse reflection from an opaque surface.

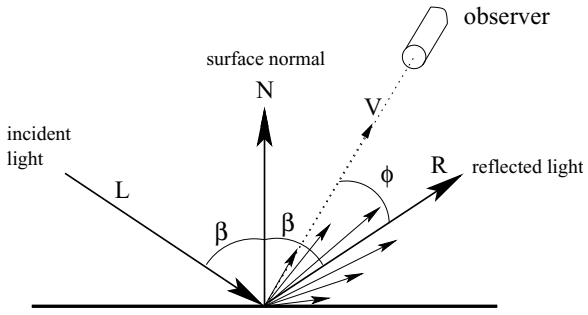

Figure 2: Specular reflection from an opaque surface.

In perfect or specular (mirror–like) reflection, the incident light is reflected in the plane defined by the incident light and the surface normal, making an angle with the surface normal, which is equal to the incidence angle (Fig. 2).

Phong illumination model [4], which is frequently used in computer graphics applications, combines the three types of reflection, which are ambient, diffuse, and specular reflection, in a single formula:

$$I = I_a k_a + I_i[k_d(\vec{L}.\vec{N})] + I_i[k_s(\vec{R}.\vec{V})^n] \tag{2}$$

where I_a and I_i are the intensities of ambient and incident light, k_a, k_d, and k_s are the coefficients of ambient light, diffuse, and specular reflection for a given material, and $\vec{L}$, $\vec{N}$, $\vec{R}$, and $\vec{V}$ are the unit vectors representing light source, surface normal, reflected light, and viewing direction, respectively, as shown in Fig. 2. The ambient reflection component,

This research was supported by TÜBİTAK under BDP and 197E051 grants. The authors would like to thank the Robotics Research Group of the University of Oxford for donating the infrared sensors.

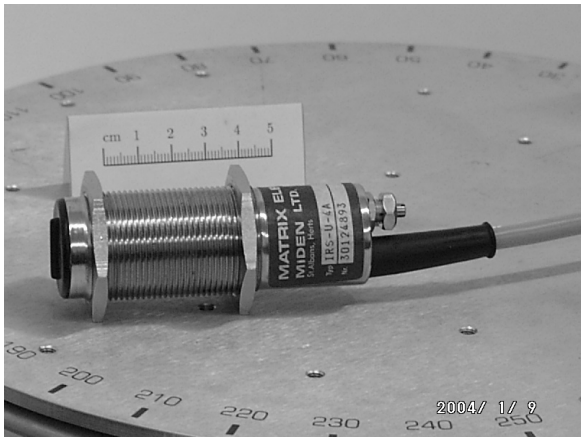

Figure 3: Close-up view of the infrared sensor.

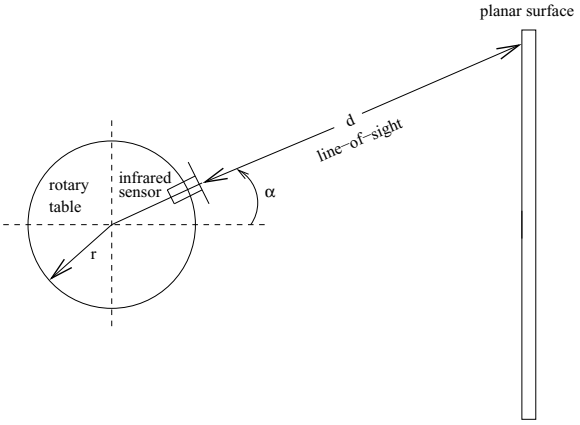

Figure 4: Top view of the experimental setup. The emitter and detector windows are circular with 8 mm diameter and center-to-center separation 12 mm. (The emitter is above the detector.) Both the scan angle α and the target azimuth θ are measured counter-clockwise from the horizontal axis.

which is the first term in Equation (2), can be neglected with respect to the other terms because the infrared filter, covering the detector window, filters out this term.

In [5], the simple nonempirical mathematical model described above is used to model reflections from planar surfaces located at known distances by fitting the reflectance data to the model represented by Equation (2) and improvements are made in the range estimates of infrared sensors. Our approach differs from that in [5], in that it uses a simpler model, takes distance as a variable, and does not require prior knowledge of the distance. Another difference is that, the study [5] concentrates mainly on range estimation for a limited range interval rather than determination of the surface type whereas in this study, we focus on the determination of the surface type. We also note that the position-invariant pattern recognition and position estimation achieved in this paper is different from such operations performed on conventional images [6] in that here we work not on direct "photographic" images of the surfaces obtained by some kind of imaging system, but rather on intensity scan signals obtained by rotating a point sensor. As such, position invariant differentiation and localization is achieved with an approach quite different than those employed in invariant pattern recognition and localization in conventional images. In [7], the recognition capabilities of active infrared sensor arrays are analyzed by simulation of infrared signal propagation using the model represented by Equation (2). In our earlier work, we considered the differentiation and localization of objects with different geometries such as plane, corner, edge, and cylinder with infrared sensors using nonparametric [8] and rule–based [9] approaches. In [10], surfaces of different properties are differentiated and localized with infrared sensors using nonparametric approaches.

This paper is organized as follows: In Section 2, the parametric modeling of infrared intensity signals is discussed. Section 3 provides experimental verification of the approach presented in this paper. Concluding remarks are made in the last section.

2. MODELING OF INFRARED INTENSITY SIGNALS

The surface materials considered are wood, styrofoam packaging material, white painted wall, white and black clothes, and white, brown, and violet papers. The infrared sensor [11] (see Fig. 3) is mounted on a 12 inch rotary table [12] (Fig. 4) to obtain angular intensity scan signals from these surfaces. Reference intensity scan signals are collected for each surface type by locating the surfaces with 2.5 cm distance increments, ranging from 30 cm to 52.5 cm, at $\theta = 0^\circ$. An example of resulting reference scan signals is shown in Fig. 5 for styrofoam packaging material using dotted lines. These intensity scans have been modeled by approximating the surfaces as ideal Lambertian surfaces. The received return signal intensity is modeled as

$$\mathcal{I} = \frac{C_0 \cos(\alpha C_1)}{\left[\frac{C_2}{\cos(\alpha)} + r\left(\frac{1}{\cos(\alpha)} - 1\right)\right]^2} \tag{3}$$

which is a modified version of the second term in the model represented by Equation (1). Here, C_0 is a constant due to the reflection coefficient of the surface, C_1 is a term added to compensate the change in the basewidth of the intensity scans with respect to distance (Fig. 5), and C_2 is the horizontal distance between the rotary platform and the surface. A similar dependency on C_1 is used in sensor modeling in [13]. The denominator of $\mathcal{I}$ is the distance d between the infrared sensor and the surface, which can be easily seen from Fig. 4.

Based on the model represented by Equation (3), parameterized curves have been fitted to the reference intensity scan signals by using a nonlinear least-squares method [14]. Resulting curves are shown in Fig. 5 in solid lines for the styrofoam packaging material. The fitted curves for the other surfaces have similar characteristics. For the reference scans, C_2 is not taken as a parameter since we already know the distance of the surface to the infrared sensing unit. The initial guesses must be made cleverly so that the algorithm does not converge to local minima and curve fitting is achieved in a smaller number of iterations. The initial guess for C_0 is made by evaluating $\mathcal{I}$ at $\alpha = 0^\circ$, which is the product of $\mathcal{I}$ with d^2 at $\alpha = 0^\circ$. Similarly, the initial guess for C_1 is made by evaluating C_1 from Equation (3) at a known angle α other than zero, with the initial guess C_0 and known range d at $\alpha = 0^\circ$. While curve fitting, C_0 value is allowed to vary

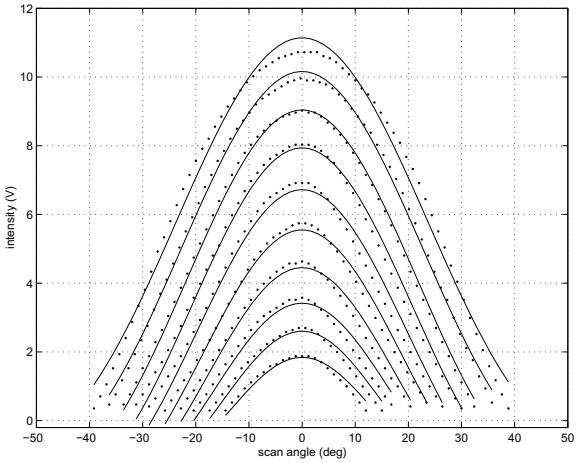

Figure 5: Intensity scan signals of styrofoam packaging material at different distances. Solid lines indicate the model fit and the dotted lines indicate the actual data.

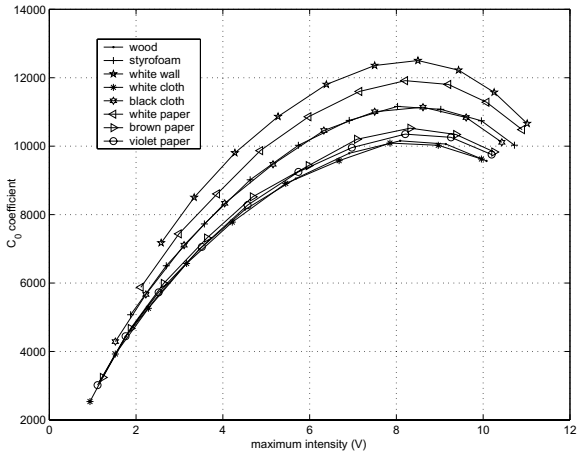

Figure 6: Variations of the parameter C_0 with respect to the maximum intensity of the scan signal.

between $\pm$ 2000 of its initial guess and C_1 is restricted to be positive. The variations of C_0, C_1, and C_2 (or d at $\alpha = 0°$) with respect to the maximum intensity of the reference scans are shown in Figs. 6–8. As the distance d increases, C_0 decreases and C_1 increases as expected from the model represented by Equation (3). The model fit is much better for scan signals with smaller maximum intensities because the contribution of the specular reflection components around the maximum value of the intensity scans increases as the distance decreases and our model takes only diffuse reflections into account. Therefore, the error between the actual data and fitted curve increases beyond a certain distance as shown in Fig. 5. This effect can be seen in the C_0 coefficient (Fig. 6), where C_0 value begins to decrease beyond a certain range. However, the same effect cannot be observed in the variation of C_1 (Fig. 7), which is critical in our decision process. The operating range of our approach is extended at the expense of the error in curve fitting at smaller ranges.

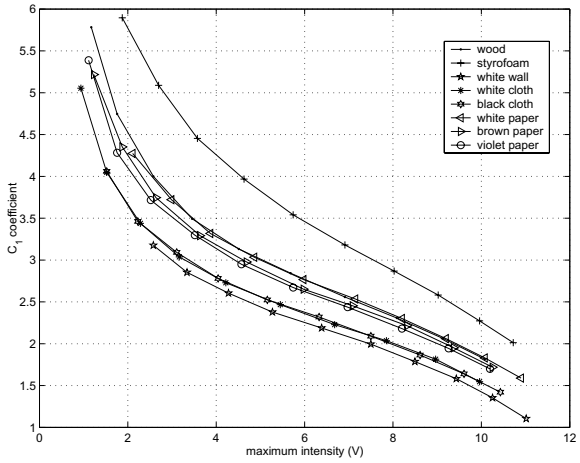

Figure 7: Variations of the parameter C_1 with respect to the maximum intensity of the scan signal.

3. EXPERIMENTAL VERIFICATION AND DISCUSSION

In this section, we experimentally verify the proposed method. In the test process, the surfaces are randomly located at azimuth angles varying from $-45°$ to $45°$ and ranges from 30 cm to 52.5 cm, where the return signal intensities do not saturate. Firstly, the maximum intensity of the observed intensity scan is found and the angular value, where this maximum occurs, is taken as the azimuth estimate of the surface. If there are multiple maximum intensity values, the average value of the minimum and maximum angular values, where the maximum intensity values occur, is calculated to find the azimuth estimate of the surface. The observed scan is shifted by the azimuth estimate and the model represented by Equation (3) is fitted using nonlinear least-squares method. Initial guesses for C_0 and C_1 are made in the same way as explained before for the reference scans. The initial guess for distance C_2 is found by taking the average of the maximum possible and the minimum possible range values corresponding to the maximum value of the recorded intensity scan. These values are found from Fig. 8 by linear interpolation. This results in

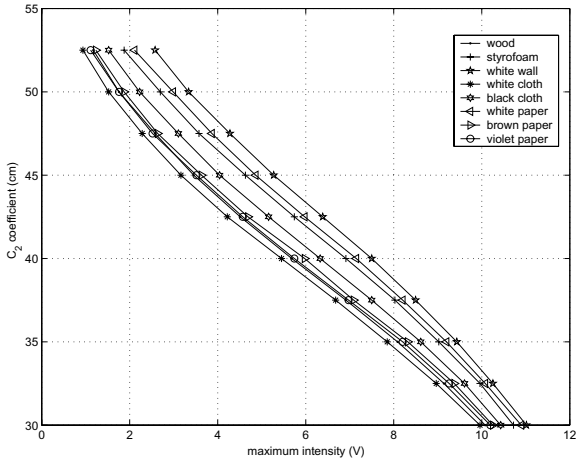

Figure 8: Variations of the parameter C_2 (or d at $\alpha = 0°$) with respect to the maximum intensity of the scan signal.

a maximum absolute range error of approximately 2.5 cm. The parameter C_2 is allowed to vary between ± 2.5 cm of its initial guess. After nonlinear curve fitting to the observed scan, we get three parameters C_0^*, C_1^*, and C_2^*. In the decision process, the maximum intensity of the observed scan is used and a value of C_1 is obtained by linear interpolation on Fig. 7 for each surface type. Decisions are taken based on the absolute difference of $C_1 - C_1^*$ because of the distinctive nature of the C_1 variation with respect to the maximum intensity. The surface type giving the minimum error is chosen as the correct surface type. This might be also done by comparing the parameters with those at the estimated range. However, this does not give better results because of the error and uncertainty in the range estimates C_2.

The surface recognition results are tabulated in Table 1. An overall correct differentiation rate of 73% over eight different surfaces is achieved and surfaces are located with absolute range and azimuth errors of 0.8 cm and 1.1^o, respectively. Four of these surface types, which are styrofoam, white painted wall, and brown and violet paper, can be correctly classified with 100% accuracy. White and black clothes are confused with each other. Similarly, wood and white paper are confused with each other with only one exception. We can reduce the number of surfaces differentiated and get higher differentiation rates. For example, if we exclude black cloth from our test set, we get a correct differentiation rate of 86%. Similarly, if we form a set of surfaces excluding wood and white cloth or wood and black cloth, we get a correct differentiation rate of 100% for the remaining six surfaces, and the surfaces are located with absolute range and azimuth errors of 0.2 cm and 1.1^o and 0.3 cm and 1.1^o, respectively.

Table 1: Surface confusion matrix: C_1-based recognition. (WO: wood, ST: styrofoam, WW: white wall, WC: white cloth, BC: black cloth, WP: white paper, BR: brown paper, VI: violet paper).

surface	recognition result								total
	WO	ST	WW	WC	BC	WP	BR	VI	
WO	4	–	–	–	–	7	–	1	12
ST	–	12	–	–	–	–	–	–	12
WW	–	–	12	–	–	–	–	–	12
WC	–	–	–	7	5	–	–	–	12
BC	–	–	–	9	3	–	–	–	12
WP	4	–	–	–	–	8	–	–	12
BR	–	–	–	–	–	–	12	–	12
VI	–	–	–	–	–	–	–	12	12
total	8	12	12	16	8	15	12	13	96

4. CONCLUSION

In this study, we achieve location-invariant surface recognition by processing and modeling the intensity scan signals obtained with simple, low-cost infrared sensors. The proposed approach can differentiate six different surfaces with 100% accuracy. In [10], where we considered differentiation and localization of surfaces by nonparametric approaches, a maximum correct differentiation rate of 87% over four surfaces was achieved. Comparing this rate with that obtained in this study, we can conclude that parametric approach is superior to nonparametric one, in terms of the accuracy, number of surfaces considered, and memory requirements, where the latter one requires the storage of reference scan signals.

The proposed method can be used in industrial applications where different surfaces must be identified and separated in a cost effective way and in mobile robot applications for recognition of the surfaces at nearby ranges.

Current and future work involves modeling of saturated scans, hence extending the operating range of our approach and extension of the model by including specular reflections. We also plan to consider surface recognition by the use of artificial neural networks in order to improve the accuracy of the system.

REFERENCES

[1] M. D. Adams, "Lidar design, use, and calibration concepts for correct environmental detection," *IEEE Trans. Robot. Automat.*, vol. 16, no. 6, pp. 753–761, Dec. 2000.

[2] X. D. He, K. E. Torrance, F. X. Sillion, and D. P. Greenberg, "A comprehensive physical model for light reflection," *Computer Graphics*, vol. 25, no. 4, pp. 175–186, Jul. 1991.

[3] E. R. Davies, *Machine Vision: Theory, Algorithms, Practicalities*, London: Academic Pr., 1990.

[4] B. T. Phong, "Illumination for computer generated pictures," *Commun. ACM*, vol. 18, no. 6, pp. 311–317, Jun. 1975.

[5] P. M. Novotny and N. J. Ferrier, "Using infrared sensors and the Phong illumination model to measure distances," in *Proc. IEEE Int. Conf. Robot. Automat.*, Detroit, MI, May 1999, pp. 1644–1649.

[6] F. T. S. Yu and S. Jutamulia, ed., *Optical Pattern Recognition*, Cambridge: Cambridge University Press, 1998.

[7] B. Iske, B. Jäger, and U. Rückert, "A ray-tracing approach for simulating recognition abilities of active infrared sensor arrays," in *Proc. IEEE Int. Conf. Sensors*, Orlando, Florida, Jun. 2002, vol. 2, pp. 1227–1232.

[8] T. Aytaç and B. Barshan, "Differentiation and localization of targets using infrared sensors," *Opt. Commun.*, vol. 210, no. 1–2, pp. 25–35, Sept. 2002.

[9] T. Aytaç and B. Barshan, "Rule-based target differentiation and position estimation based on infrared intensity measurements," *Opt. Eng.*, vol. 42, no. 6, pp. 1766–1771, Jun. 2003.

[10] B. Barshan and T. Aytaç, "Position-invariant surface recognition and localization using infrared sensors," *Opt. Eng.*, vol. 42, pp. 3589–3594, Dec. 2003.

[11] Matrix Elektronik, AG, Kirchweg 24 CH-5422 Oberehrendingen, Switzerland, *IRS-U-4A Proximity Switch Datasheet*, 1995.

[12] Arrick Robotics, P.O. Box 1574, Hurst, Texas, 76053, URL: www.robotics.com/rt12.html, *RT-12 Rotary Positioning Table*, 2002.

[13] G. Petryk and M. Buehler, "Dynamic object localization via a proximity sensor network," in *Proc. IEEE/SICE/RSJ Int. Conf. Multisensor Fusion Integration for Intelligent Systems*, Washington DC, Dec. 1996, pp. 337–341.

[14] *Numerical Recipies in C: The Art of Scientific Computing*, Cambridge University Press, URL:www.library.cornell.edu/nr/bookcpdf.html.